

Harnessing subspace controllability: Time-optimal Dicke-state generation in Heisenberg-coupled qubit arrays with a single local control

Vladimir M. Stojanović,¹ Tommaso Calarco,^{2,3,4} and Andrea Muratori²

¹*Institut für Angewandte Physik, Technical University of Darmstadt, D-64289 Darmstadt, Germany*

²*Dipartimento di Fisica e Astronomia, Università di Bologna, 40127 Bologna, Italy*

³*Forschungszentrum Jülich GmbH, Peter Grünberg Institute,*

Quantum Control (PGI-8), 52425 Jülich, Germany

⁴*Institute for Theoretical Physics, University of Cologne, Zülpicher Straße 77, 50937 Cologne, Germany*

(Dated: January 1, 2026)

We explore the feasibility of realizing Dicke states in qubit arrays with always-on isotropic Heisenberg coupling between adjacent qubits, assuming a single Zeeman-type control acting in the z direction on an actuator qubit. The Lie-algebraic criteria of controllability imply that such an array is not completely controllable, but satisfies the conditions for subspace controllability on any subspace with a fixed number of excitations. Therefore, a qubit array described by the model under consideration is state-to-state controllable for an arbitrary choice of initial and final states that have the same Hamming weight. This limited controllability is exploited here for the time-optimal dynamical generation of an a -excitation Dicke state $|D_a^N\rangle$ ($a = 1, 2, \dots, N-1$) in a linear array with N qubits starting from a generic Hamming-weight- a product state. To dynamically generate the desired Dicke states – including W states $|W_N\rangle$ as their special ($a = 1$) case – in the shortest possible time with a single local Z control, we employ an optimal-control scheme based on the *dressed Chopped RAndom Basis* (dCRAB) algorithm. We optimize the target-state fidelity over the expansion coefficients of smoothly-varying control fields in a truncated random Fourier basis; this is done by combining Nelder-Mead-type local optimizations with the multistart-based clustering algorithm that facilitates searches for global extrema. In this manner, we obtain the optimal control fields for Dicke-state preparation in arrays with up to $N = 9$ qubits. Based on our numerical results, we find that the shortest possible state-preparation times scale quadratically with N . Finally, we demonstrate the robustness of our control scheme against small control-field deviations from the optimal values.

I. INTRODUCTION

Introduced in the context of the phenomenon of superradiance [1], Dicke states have in recent years been extensively investigated in connection with a variety of emerging quantum-technology applications. To be more specific, favorable properties of this class of highly-entangled multiqubit states [2] – above all, their extreme robustness to particle loss [3, 4], their immunity to collective dephasing noise [5], as well as their permutationally-symmetric character [6] – make them a viable candidate for applications in areas as diverse as quantum game theory [7], quantum networking [8], quantum metrology [9, 10], quantum error correction [11], and quantum combinatorial optimization [12], to name but a few.

Motivated by their anticipated promise in the realm of quantum technology, Dicke states have already been realized in several classes of physical systems. In addition, a multitude of proposals for the realization of those states in diverse physical systems were put forward in the past. Examples are furnished by trapped ions [13–15], neutral atoms [16–19], photons [8, 20], and superconducting qubits [21]. It should be stressed, however, that most of the demonstrated schemes for the realization of Dicke states – as well as the existing theoretical proposals for their realization – allow one to engineer only particular instances of those states, rather than an arbitrary state from this family [22]. Furthermore, most of the envisioned state-preparation schemes are fraught with some

additional limitations – for example, they require specific initial states (e.g. a Fock state) or individual qubit addressing as a prerequisite for realizing Dicke states.

In this paper, the feasibility of dynamical generation of Dicke states is investigated in the special case of linear qubit arrays with nearest-neighbor Heisenberg-type coupling and a single local control. This nontrivial quantum-state-engineering problem is addressed here by making use of the Lie-algebraic controllability criteria [23–26] and employing the optimal-control methods [27–30]. While the former guarantee the existence of time-dependent control fields that render the envisioned state-engineering scheme possible – but without specifying the actual time dependence of those fields – the latter can be utilized to determine the sought-after time dependence [31–33].

It is well-understood by now that the Heisenberg interaction between qubits by itself does not suffice for universal QC [34], by contrast to the Ising- and XY -type interactions. It has been demonstrated, however, that universal QC can still be realized with the Heisenberg interaction alone if encoded qubit states – with the role of logical qubits being played by triples [34] or pairs [35] of physical qubits – are introduced, leading to the concept of encoded universality [36]. Another useful insight as to the potential relevance of this type of qubit-qubit coupling – which was also discussed in the context of measurement-based QC [37] and stabilizer codes [38] – within the circuit model of QC came from Lie-algebraic studies of interacting spin-1/2 chains acted upon by time-dependent

control fields [39, 40]. To be more specific, it was shown that a spin-1/2 chain with an “always-on” Heisenberg-type interaction is completely controllable provided that at least two noncommuting controls – e.g., a Zeeman-type magnetic field with nonzero components in two mutually orthogonal directions (e.g., x and y) that act on a single spin (qubit) [40]. Under this condition, an arbitrary quantum gate can in principle be realized in this array [41, 44, 45], which is equivalent to universal QC.

The fact that two local controls – that need not act on the same qubit [40] – are already sufficient for complete controllability of a Heisenberg-coupled N -qubit array begs the question whether an even smaller control resource permits some semblance of controllability in such an array. Indeed, it has already been shown that a single local control in such an array guarantees subspace controllability [43] on an arbitrary subspace of the total Hilbert space that is characterized by a fixed number a of excitations [40]. This also implies state-to-state controllability on each of those $N + 1$ subspaces. In other words, for an arbitrary choice of initial- and final states with the same number of excitations (i.e. the same Hamming weight) it is possible to find control fields such that the total system dynamics – resulting from the Heisenberg drift Hamiltonian and the control field – allows an evolution of the system from the given initial- to the desired final state.

The above Lie-algebraic results allow one to harness subspace controllability of Heisenberg-coupled qubit array with a single local control in the form of an analog (pulse-level) Dicke-state engineering scheme. Namely, given that the Dicke state with a certain excitation number a is the equal-weight linear combination of all possible product states with the same number of excitations, this Dicke state is reachable in the system at hand provided that one starts from a generic product state with the Hamming weight a . In other words, starting from an initial product state with a excitations at time $t = 0$, the a -excitation Dicke state can be dynamically generated at some later time $t = T$. To find the appropriate time-dependence of the control field that allows one to steer the system towards the desired Dicke state as rapidly as possible, i.e. in the shortest possible time T , the toolbox of quantum optimal control is employed here.

The control scheme utilized here for Dicke-state engineering relies on smoothly-varying control fields expanded over a truncated random Fourier basis of functions. The global maxima of the relevant figure of merit (target-state fidelity) as a function of the expansion coefficients of the control field are obtained by combining a Nelder-Mead type local-optimization method [47] and the multistart-based clustering algorithm that facilitates the search for global extrema [48]. In this manner, both the shortest possible times required for high-fidelity realizations of Dicke and W states, as well as the corresponding optimal control fields, are obtained.

The remainder of this paper is structured as follows. To begin with, the definition and basic properties of

Dicke states are reviewed in Sec. II. In Sec. III the main Lie-algebraic results pertaining to the controllability of spin-1/2 chains with nearest-neighbor Heisenberg-type coupling are recapitulated. The following, Sec. IV covers in detail the subspace controllability of the same class of systems. Section V specifies the system under investigation and the control objectives, as well as describing in detail the methodology for finding optimal control fields. The main findings of this work are presented and discussed in detail in Sec. VI. Finally, the paper is rounded out in Sec. VII, which also contains a brief summary of its principal findings.

II. DICKE STATES: AN OVERVIEW

To set the stage for further considerations, the definition, basic properties, and concrete examples of Dicke states are provided below.

An a -excitation product state of an N -qubit system can be parameterized in the form $|\{n_1, \dots, n_a\}\rangle$, where n_1, \dots, n_a enumerate the qubits that are in the logical state $|1\rangle$ and the remaining qubits are in the state $|0\rangle$. The N -qubit Dicke state with a excitations is given by the equal-weight superposition of all the product states $|\{n_1, \dots, n_a\}\rangle$, i.e.

$$|D_a^N\rangle = \binom{N}{a}^{-1/2} \sum_{n_1 < \dots < n_a}^N |\{n_1, \dots, n_a\}\rangle. \quad (1)$$

In other words, the N -qubit Dicke states with a excitations is the equal-weight linear combination of the $\binom{N}{a}$ product states corresponding to the bit strings of Hamming weight a .

In the special, single-excitation ($a = 1$) case Dicke states coincide with W states, i.e. $|D_1^N\rangle \equiv |W_N\rangle$, where

$$|W_N\rangle = \frac{1}{\sqrt{N}} (|10\dots0\rangle + |010\dots0\rangle + \dots + |000\dots1\rangle). \quad (2)$$

is the N -qubit W state. W states constitute one of the most important classes of maximally-entangled multiqubit states and have many generalizations. Being more robust to particle loss than any other class of multiqubit states, W states hold promise for a multitude of quantum-technology applications; as a result, their realizations are proposed in all currently investigated physical platforms for QC [49–52].

Instead of the notation used in the above definition of Dicke states [cf. Eq. (1)], for small N it is more convenient to use a simpler notation that involves binary bit strings. For example, the two-excitation ($a = 2$) Dicke state $|D_2^3\rangle$ in a system of $N = 3$ qubits, and its counterpart $|D_2^4\rangle$ in an 4-qubit system, are given by

$$\begin{aligned} |D_2^3\rangle &= \frac{1}{\sqrt{3}} (|110\rangle + |101\rangle + |011\rangle), \\ |D_2^4\rangle &= \frac{1}{\sqrt{6}} (|1100\rangle + |1010\rangle + |1001\rangle \\ &\quad + |0110\rangle + |0101\rangle + |0011\rangle). \end{aligned} \quad (3)$$

It is important to note that N -qubit Dicke states are invariant under arbitrary permutations of qubits. This property is manifest in yet another useful representation of Dicke states, equivalent to Eq. (1), which is given by

$$|D_a^N\rangle = \binom{N}{a}^{-1/2} \sum_P P\{|1\rangle^{\otimes a} |0\rangle^{\otimes(N-a)}\}, \quad (4)$$

where the sum on the RHS of the last equation runs over all permutations P of the set $\{1, 2, \dots, N\}$. Moreover, Dicke states $|D_a^N\rangle$ ($a = 0, \dots, N$) form a basis of the permutationally-invariant subspace (the symmetric sector) of the 2^N -dimensional N -qubit Hilbert space; the fact that this last subspace has the dimension $N + 1$, which grows only linearly – rather than exponentially – with the number of qubits, explains its widespread use in quantum-information problems involving fully permutationally-invariant systems [53–57].

For completeness, it is worthwhile mentioning that deterministic preparation of Dicke states based on a quantum circuit that consists of single- and two-qubit gates has been proposed [58]. In that circuit, both the depth and the gate-count scale linearly, i.e. as $\mathcal{O}(N)$, with the number of qubits; because of this favorable scaling, Dicke states are often utilized as initial states in quantum-optimization algorithms. In the special case of qubit arrays with all-to-all connectivity, for the state $|D_a^N\rangle$ this last linear scaling can be improved to $\mathcal{O}(a \log \frac{N}{a})$ [59].

III. CONTROLLABILITY / REACHABILITY FOR HEISENBERG SPIN-1/2 CHAINS

In what follows, a survey of the principal Lie-algebraic results pertaining to Heisenberg-coupled qubit arrays is given, with emphasis on those of direct interest for the present work. The general Lie-algebraic framework of quantum control is first reviewed (Sec. III A). This is followed by a general introduction into the concept of local control (Sec. III B). Basic results pertaining to minimal control resources required for complete controllability of Heisenberg-coupled arrays are then discussed (Sec. III C).

Before embarking on discussions of general controllability and reachability criteria, as well as their applications to interacting spin-1/2 chains (qubit arrays), it is pertinent to introduce the notation that will be used in what follows for writing Hamiltonians of such systems. In particular, the single-qubit Pauli operators will be denoted by X , Y , and Z ; using the standard computational basis, these operators can be expressed as $X \equiv |0\rangle\langle 1| + |1\rangle\langle 0|$, $Y \equiv i(|1\rangle\langle 0| - |0\rangle\langle 1|)$, and $Z \equiv |0\rangle\langle 0| - |1\rangle\langle 1|$, while $\mathbb{1}_2 = |0\rangle\langle 0| + |1\rangle\langle 1|$ is the single-qubit identity operator [60]. The counterparts of the operators X , Y , and Z that act in the N -qubit Hilbert space $\mathcal{H} \equiv (\mathbb{C}^2)^{\otimes N}$ (the tensor product of single-qubit Hilbert spaces \mathbb{C}^2) will be denoted by X_n , Y_n , and Z_n , respectively, in the following. These last operators are

jointly defined by the tensor-product relation

$$\mathbf{X}_n \equiv \mathbb{1}_2 \otimes \dots \otimes \mathbb{1}_2 \otimes \underbrace{\mathbf{X}}_n \otimes \mathbb{1}_2 \otimes \dots \otimes \mathbb{1}_2, \quad (5)$$

where $\mathbf{X} \equiv (X, Y, Z)^T$ is the vector of single-qubit Pauli operators and $\mathbf{X}_n \equiv (X_n, Y_n, Z_n)^T$ ($n = 1, \dots, N$) that of their extension to the N -qubit Hilbert space.

A. Lie-algebraic controllability and reachability criteria for finite-dimensional quantum systems

Let us consider a quantum system, with the d -dimensional Hilbert space \mathcal{H} . Assume that H_0 is the time-independent intrinsic (drift) Hamiltonian of this system and that the latter is acted upon by external control fields $f_j(t)$ ($j = 1, \dots, p$). These fields couple to certain degrees of freedom of the system, which are represented by Hermitian operators H_j . The total Hamiltonian of the system is then given by

$$H(t) = H_0 + \sum_{j=1}^p f_j(t) H_j. \quad (6)$$

The time-evolution operator $U(t)$ of the system satisfies the time-dependent Schrödinger equation ($\hbar = 1$)

$$\frac{dU}{dt} = -i[H_0 + \sum_{j=1}^p f_j(t) H_j] U(t), \quad (7)$$

with the initial condition $U(t = 0) = \mathbb{1}_d$, where $\mathbb{1}_d$ is the identity operator on the Hilbert space \mathcal{H} [26]. The objective of a generic quantum-control problem is to determine a time $T > 0$ and time-dependent controls $f_j(t) \in \mathbb{R}$ such that a desired unitary U_{target} is reached at $t = T$; in other words, $U(t = T) = U_{\text{target}}$. In particular, the system is said to be completely (operator) controllable provided that its dynamics, governed by $H(t)$, gives rise – with a certain choice of the fields $f_j(t)$ – to an arbitrary unitary on its Hilbert space. Rephrasing, complete controllability assumes that the reachable set of the system – i.e., the set of unitaries achievable by varying the controls – is given by the Lie group $U(d)$ or $SU(d)$ [26].

The criteria of controllability for quantum systems are framed using Lie-algebraic concepts [23–26], among which that of the dynamical Lie algebra (DLA) of the system plays the principal role [26]. For a system governed by the Hamiltonian in Eq. (6), the DLA \mathcal{L} is generated by the skew-Hermitian counterparts of the operators H_k , i.e. by the operators $\{-iH_k | k = 0, \dots, p\}$. The necessary and sufficient condition for complete controllability (the Lie-algebraic rank condition) [26] is that \mathcal{L} be isomorphic to the Lie algebra $u(d)$ of skew-Hermitian $d \times d$ matrices, or its counterpart $su(d)$ that corresponds to traceless skew-Hermitian ones [61]. This general result constitutes an existence theorem that guarantees that any unitary on the Hilbert space of the system is reachable for appropriately chosen control fields. Another, completely separate,

question is how to find the actual time dependence of control fields that allows one to realize a desired unitary. This is typically done by taking into account various additional constraints – for example, the one pertaining to the total duration of the control.

B. Local (quantum) control: general concept and its application to qubit arrays

The principal control-related issue pertaining to interacting quantum systems is whether a given system can be fully- or, at least, partially controlled by solely acting on its subsystem. This is the idea of the *local-control* approach, which assumes that only a small subsystem of the original system is subject to control fields. The actual choice of the subsystem crucially depends on the type of interaction in the considered quantum system.

Let us consider a composite system $S = C \cup \bar{C}$, described by the Hamiltonian

$$H(t) = H_S + \sum_j f_j^C(t) H_j^C, \quad (8)$$

where H_S is the drift part (acting on the whole system S), while H_j^C are local Hamiltonians (acting only on the subsystem C) and $f_j^C(t)$ the corresponding time-dependent control fields (for an illustration, see Fig. 1). Assuming, for simplicity, that $-iH_j^C$'s generate the Lie algebra $\mathcal{L}(C)$ on C , the system S is completely controllable iff $-iH_S$ and $-iH_j^C$ generate $\mathcal{L}(S)$, i.e.,

$$\langle iH_S, \mathcal{L}(C) \rangle = \mathcal{L}(S), \quad (9)$$

where $\langle A, B \rangle$ stands for the algebraic closure of the operator sets A and B [61]. Therefore, any unitary on S can be enacted through control of its subsystem C iff every element of $\mathcal{L}(S)$ can be obtained either as linear combinations of $-iH_S$, $-iH_j^C$, or their repeated commutators.

Qubit arrays constitute a prototypical class of systems in which local-control approach may be advantageous [62]. In keeping with the above Lie-algebraic criteria (cf. Sec. III A), complete controllability of an N -qubit array is that its corresponding DLA be isomorphic with either $u(2^N)$ or $su(2^N)$. The conventional approach to control in a qubit array requires control fields to act on each qubit in the array. Along with a drift Hamiltonian, which describes qubit-qubit interactions that make it possible to realize entangling two-qubit gates, this – in principle – permits the realization of an arbitrary (multi-qubit) gate. In contrast to this scenario, in the local-control case control fields act only on a handful of *actuator* qubits – in the extreme case, a single qubit. The specific choice of actuator qubits in a given system should ideally be one guaranteeing complete controllability, as the latter renders universal QC possible [26].

The usefulness of local control in qubit arrays cannot be overstated, especially in the context of solid-state qubits. In principle, global-control approaches to

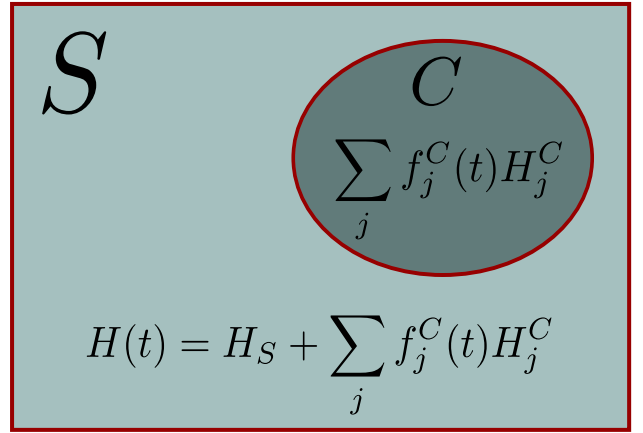


FIG. 1: Pictorial illustration of the concept of local control. System S is described by the drift Hamiltonian H_S . The system is subject to external control fields $f_j^C(t)$, which couple only to its degrees of freedom that belong to the subsystem C ; these degrees of freedom are described by the local Hamiltonians H_j^C . The total Hamiltonian of the system is then the one given by Eq. (8).

qubit arrays constitute a promising pathway to scalable QC [63]. In particular, a continuous-wave global field permits decoupling of the qubits from background noise. In the case of solid-state qubits this approach is, however, compromised by the unavoidable variability in the parameters of individual qubits in the array (e.g. statistical scatter in qubit resonance frequency). Therefore, applications of global-control strategies in solid-state QC platforms usually require additional nontrivial contingencies [64, 65], especially in large scale systems [66].

C. Complete controllability of Heisenberg-coupled spin-1/2 chains (qubit arrays): principal results

The issue of identifying the minimal control resources required for complete controllability of various interacting spin-1/2 models (Ising, XY , Heisenberg, etc.) was studied extensively in the past [39, 40]. For each of these models, the smallest subsystem was sought that – when acted upon by Zeeman-type external controls – renders the entire chain completely controllable. As it turned out, only for Heisenberg-type coupling these investigations returned nontrivial results.

The most general controllability-related result for spin-1/2 chains (qubit arrays) with Heisenberg-type interaction was proven based on a method that makes use of the Hilbert-space decomposition into a tensor product of minimal invariant subspaces [40]. This result asserts that the existence of two mutually noncommuting local controls – which need not act on the same spin (qubit) – guarantees complete controllability of the chain; importantly, this last result holds even when for fully anisotropic XYZ coupling case [40], i.e., for the drift

Hamiltonian

$$H_{XYZ} = \sum_{n=1}^{N-1} (J_x X_n X_{n+1} + J_y Y_n Y_{n+1} + J_z Z_n Z_{n+1}), \quad (10)$$

where J_x , J_y , and J_z are the three coupling strengths. While the last controllability-related result does not require the two noncommuting controls to act on the same qubit, the simplest scenario to which this theorem applies is the one in which the first qubit in the array is subject to a Zeeman-type field control field $\mathbf{B}_1(t)$ with two nonzero components. Assuming, for definiteness, that these components are x and y , i.e. that $\mathbf{B}_1(t) \equiv [B_{1x}(t), B_{1y}(t), 0]^T$, the corresponding control Hamiltonian is given by

$$H_c(t) = B_{1x}(t)X_1 + B_{1y}(t)Y_1. \quad (11)$$

The stated general controllability result, pertaining to the drift Hamiltonian H_{XYZ} [cf. Eq. 10], has two special cases that had been proven long before the general one.

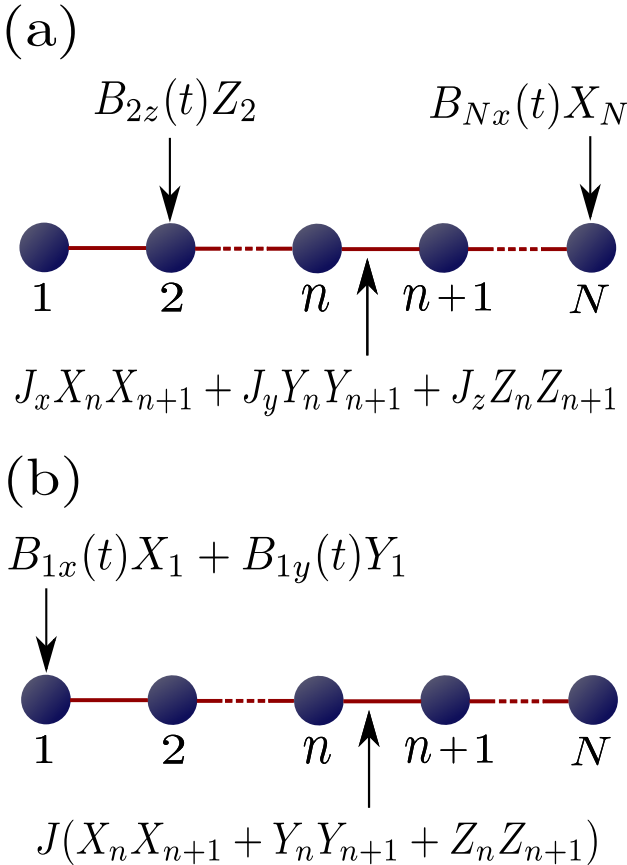


FIG. 2: Schematic illustration of possible complete-controllability scenarios in Heisenberg-coupled N -qubit arrays with a local control: (a) In an array with the fully anisotropic Heisenberg interaction a local Z control is applied to qubit 2 and local X control to qubit N , (b) In an array with the isotropic Heisenberg interaction local X - and Y controls are both applied to qubit 1.

The first of these special cases is that of the XXZ drift Hamiltonian

$$H_{XXZ} = J \sum_{n=1}^{N-1} (X_n X_{n+1} + Y_n Y_{n+1} + \Delta Z_n Z_{n+1}), \quad (12)$$

where $J_x = J_y \equiv J$ and $J_z \equiv J\Delta$, with Δ being the anisotropy parameter. The second special case corresponds to the fully isotropic Heisenberg Hamiltonian (i.e. the one with $J_x = J_y = J_z \equiv J$)

$$H_{XXX} = J \sum_{n=1}^{N-1} (X_n X_{n+1} + Y_n Y_{n+1} + Z_n Z_{n+1}), \quad (13)$$

which happens to be of most relevance for applications in realistic qubit arrays [65].

Two extreme scenarios that permit complete controllability of Heisenberg-coupled qubit arrays are illustrated in Fig. 2. An example of a qubit array with the fully anisotropic Heisenberg interaction [cf. Eq. (10)] and two noncommuting local Zeeman-type controls applied to different qubits – more precisely, one interior qubit (qubit 2) and one of the end qubits (qubit N) – is shown Fig. 2(a). On the other hand, an example of a qubit array with the isotropic Heisenberg interaction [cf. Eq. (13)] and two noncommuting local Zeeman-type controls, both applied to same end qubit (qubit 1) is depicted in Fig. 2(b).

For each of the Hamiltonians in Eqs. (10)-(13), complete controllability of the underlying system can be proven by demonstrating that its corresponding DLA, generated by the skew-Hermitian counterparts of the drift Hamiltonian [i.e., $-iH_{XYZ}$, $-iH_{XXZ}$, $-iH_{XXX}$, for the drift Hamiltonians in Eqs. (10)-(13), respectively] and the two single-spin(qubit) Pauli operators describing noncommuting controls [e.g., $-iX_1$ and $-iY_1$ in the example of the control Hamiltonian in Eq. (11)], has the dimension equal to $d^2 - 1$ (note that each of the above drift Hamiltonians, as well as the control Pauli operators, is traceless) with $d \equiv 2^N$ being the dimension of the Hilbert space of the system. This implies that the relevant DLA is isomorphic with the Lie algebra $su(d)$ [61].

IV. SUBSPACE CONTROLLABILITY OF HEISENBERG SPIN-1/2 CHAINS

The crucial control-related concept for the remainder of this work, providing the theoretical underpinning for the optimal-control-based generation of Dicke states, is that of subspace controllability. General aspects of this concept are discussed in Sec. IV A below. The discussion in Sec. IV B specializes to subspace controllability of XXZ - and XYZ -type Heisenberg spin-1/2 chains.

A. Subspace controllability: general aspects

Among different situations that can be encountered when discussing controllability of finite-dimensional

quantum systems, subspace controllability refers to the one in which the underlying Hilbert space can be split into the direct sum of invariant subspaces and, on each of these invariant subspaces, it is possible to generate any arbitrary unitary operation using appropriately chosen control functions [40]; this also implies state-to-state controllability for any choice of initial- and final states that belong to this same subspace.

Familiar examples of subspace controllability are furnished by permutationally-symmetric networks of qubits [67] – e.g., that of all-to-all Ising(zz)-coupled qubits subject to transverse (x and y) global control fields [6, 53, 68–70], where the relevant subspace is the ($N + 1$)-dimensional permutationally-invariant subspace (symmetric sector) of the total N -qubit Hilbert space (cf. Sec. II). Another example is that of XY -coupled spin-1/2 chain (qubit array) with a single local control [cf. Sec. IV B below], where subspace controllability holds for the so-called single-excitation subspace only [40].

The existence of controllable subspaces is a common situation in cases where the system under consideration possesses dynamical symmetries [42, 43]. In the context of quantum control of a general quantum system [recall Sec. III A], with the drift Hamiltonian H_0 and p external controls described by Hamiltonians H_j ($j = 1, \dots, p$), any Hermitian operator S that is not a multiple of the identity and commutes with both H_0 and all H_j ($j = 1, \dots, p$), i.e. satisfies the condition $[H_0, S] = [H_j, S] = 0$, is called the symmetry operator of the system. It follows directly that the operators H_0, H_j ($j = 1, \dots, p$), and S can be simultaneously diagonalized.

B. Subspace controllability of XXZ - and XYZ -type Heisenberg-coupled spin-1/2 chains

The existing studies of subspace controllability of Heisenberg-coupled spin-1/2 chains showed that for this class of models subspace controllability depends on whether the (two-local) interactions in the two directions perpendicular to the control direction are equal or not, i.e., whether the spin-1/2 chain is of XXZ type – including the fully isotropic XXX case – or anisotropic XYZ type [40]. Due to the significantly higher degree of symmetry in the XXZ case, the character of dynamical symmetries – accordingly, that of invariant subspaces as well – is different in these two cases.

In the case of XXZ -type Hamiltonians [cf. Eq. (12)] – including the special case $\Delta = 1$ [i.e. the isotropic (XXX) Heisenberg Hamiltonian in Eq. (13)] – it is pertinent to introduce the excitation operator

$$S_{\text{exc}} = \frac{1}{2} \sum_{n=1}^N (\mathbb{1}_2 + Z_n). \quad (14)$$

It is worthwhile noting that this operator can be recast

as $S_{\text{exc}} = S_z + N/2$, where

$$S_z = \frac{1}{2} \sum_{n=1}^N Z_n \quad (15)$$

is the z projection of the collective-spin operator of the system. The excitation operator has $N+1$ distinct eigenvalues $a = 0, 1, \dots, N$. Therefore, the Hilbert space of the system can be decomposed as a direct sum of its eigensubspaces, i.e. $\mathcal{H} = \bigoplus_{a=0}^N \mathcal{H}_a$. In particular, the eigensubspace \mathcal{H}_a is generated by the states corresponding to bit-strings with exactly a occurrences of 1, i.e. a -excitation states (also known as Hamming-weight- a states).

It is straightforward to verify that $[H_{XXZ}, S_{\text{exc}}] = 0$. Provided that the relevant control Hamiltonians H_j contain only Pauli- Z operators, then S_{exc} commutes with all of them and defines a symmetry, which is referred to as the excitation symmetry. As a result, both the Hamiltonian H_{XXZ} and control Hamiltonians can be block-diagonalized on each of the $N + 1$ eigensubspaces \mathcal{H}_a of \mathcal{H} , which in that case also represent the invariant subspaces of the system. It is straightforward to see that for an N -qubit system, the dimension of \mathcal{H}_a is given by

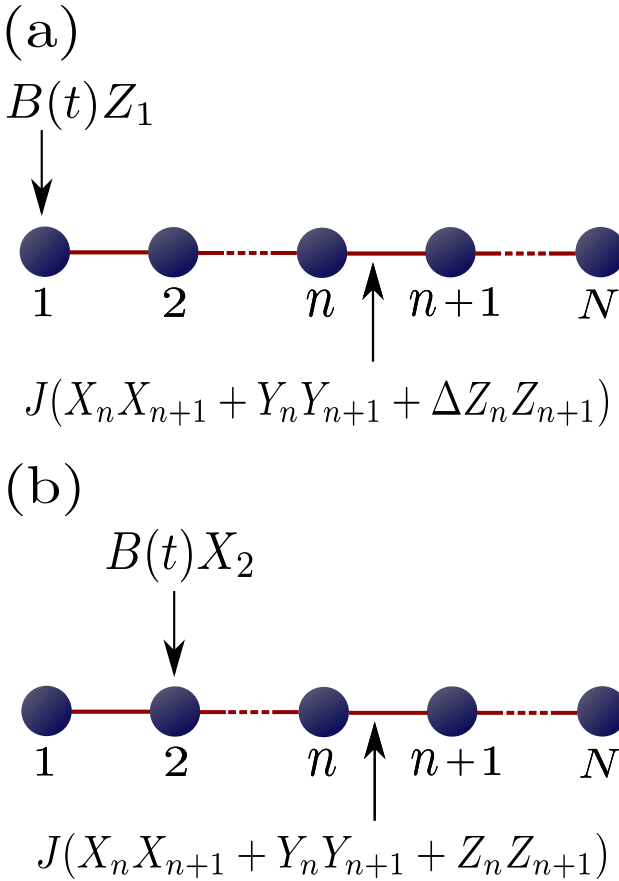
$$\dim \mathcal{H}_a = \binom{N}{a} = \frac{N!}{a!(N-a)!}. \quad (16)$$

In particular, the largest of these invariant subspaces is the one that for N even corresponds to $a = N/2$ (in the case of odd N it corresponds to $a = \lfloor N/2 \rfloor$); the asymptotic dimension of this subspace for large N grows exponentially with N [71]; namely, by making use of the Stirling formula $N! \approx \sqrt{2\pi N(N/e)^N}$ (for large N) one finds that $\dim \mathcal{H}_{N/2} \sim 2^N / \sqrt{\pi/2N}$ for large N .

As already proven in [40], an XXZ spin-1/2 chain of length N with a single local Z control on an end spin is controllable on each of the $N + 1$ invariant excitation subspaces $\mathcal{H}_0, \dots, \mathcal{H}_N$. It is important to stress that this last result also holds for the special case of an isotropic Heisenberg XXX chain. However, in the latter case, owing to the absence of preferred spatial direction (i.e. the symmetry between the x , y , and z directions), this result applies for a local control in any of the three directions.

Two possible subspace-controllability scenarios in spin-1/2 chains (qubit arrays) with XXZ -type Heisenberg interaction are illustrated in Fig. 3. While Fig. 3(a) depicts the most general XXZ -interaction case – where a single local control ought to be applied in the z direction – Fig. 3(b) illustrates the special case of isotropic Heisenberg interaction, where a control in the x direction is equally permissible as one in the z direction.

By contrast to the XXZ case, for the XYZ model [cf. Eq. (10)] the excitation symmetry [represented by the operator S_{exc} in Eq. (14)] – is not one of the dynamical symmetries. However, this model does have the Z -parity symmetry, represented by the operator $S_P = Z_1 Z_2 \dots Z_N$; H_{XYZ} has two 2^{N-1} -dimensional invariant



subspaces \mathcal{H}_1 and \mathcal{H}_{-1} , which correspond to the eigenvalues ± 1 of S_P , respectively. Therefore, compared to the XXZ case, the number of invariant subspaces in the XYZ chain is reduced from $N + 1$ to 2 as a consequence of symmetry breaking between the x and y directions. Similarly to the XXZ case, it was proven that an XYZ spin-1/2 chain of length N with a single local Z control on an end spin, the system is indeed controllable on each of the two invariant subspaces \mathcal{H}_1 and \mathcal{H}_{-1} [40].

For the sake of completeness, it is worthwhile mentioning that in the absence of the ZZ coupling [i.e. in the special case $J_z = 0$ of Eq. (10)] – i.e. for the XY -type Hamiltonians (including its special case $J_x = J_y \equiv J$, known as the XX Hamiltonian) – the subspace controllability holds only in the single-excitation subspace ($a = 1$). It is also useful to mention that an interesting class of highly-entangled multiqubit states that belong to such a subspace is that of W -type (Hamming-weight-1) states; the most important subclass of such states are the conventional, maximally-entangled W states [cf. Eq. (2)].

Without significant loss of generality, the analysis of the dynamical generation of Dicke states in the remainder of this work (see Secs. V and VI below) will be carried out only in the isotropic Heisenberg-interaction case, described by the Hamiltonian H_{XXX} . This choice is primarily motivated by the practical relevance of isotropic Heisenberg interactions in realistic qubit arrays, e.g. those based on spin qubits [65].

V. DYNAMICAL GENERATION OF DICKE STATES WITH A LOCAL CONTROL

The subspace-controllability results reviewed in Sec. IV B are utilized in the following for the dynamical generation of Dicke states in qubit arrays with the isotropic Heisenberg interaction between adjacent qubits. The connection between these subspace-controllability results and the reachability of Dicke states is explained in Sec. V A below, where the Dicke-state generation is also framed as a quantum-control problem. In Sec. V B, the methodology for solving this last problem of quantum-state control is briefly described. The adopted dCRAB approach for optimizing the principal figure of merit in the problem at hand (target-state fidelity) is then briefly described in Sec. V C.

A. Generation of $|D_a^N\rangle$ in qubit arrays with isotropic Heisenberg-type interaction

As already expounded in Sec. IV B, an array of N qubits with nearest-neighbor isotropic Heisenberg interaction and a single local control acting in x , y , or z direction satisfy the criteria for subspace controllability on any subspace \mathcal{H}_a with the fixed number a of excitations ($a = 1, 2, \dots, N - 1$). All such qubit arrays are described by time-dependent Hamiltonians of the form

$$H(t) = J \sum_{n=1}^{N-1} (X_n X_{n+1} + Y_n Y_{n+1} + Z_n Z_{n+1}) + \mathbf{B}(t) \cdot \mathbf{X}_{n_c}. \quad (17)$$

where $\mathbf{B}(t)$ stands for the unidirectional external Zeeman-type control field and $\mathbf{X}_{n_c} \equiv (X_{n_c}, Y_{n_c}, Z_{n_c})$ is the vector of Pauli operators [cf. Sec. III] corresponding to the actuator qubit $n = n_c$. For instance, $\mathbf{B}(t) = [0, 0, B(t)]$ and $n_c = 1$ correspond to the situation where qubit 1 is acted upon by a local Pauli- Z control; similarly, $\mathbf{B}(t) = [B(t), 0, 0]$ and $n_c = 2$ if qubit 2 is acted upon by a Pauli- X control.

One immediate implication of the subspace controllability of qubit arrays described by the Hamiltonians in Eq. (17) is the state-to-state controllability of such a system on each of the $N + 1$ subspaces; therefore, for an initial N -qubit state with a certain number a of excitations, any other N -qubit state with the same number

of excitations (i.e. the same Hamming weight) is reachable – through an appropriately chosen time-dependent control field – in this system.

The established reachability of an arbitrary N -qubit state with a fixed number a of excitations – from any other state with the same number of excitations – can be harnessed for the purpose of engineering Dicke states in the system under consideration. The N -qubit Dicke state $|D_a^N\rangle$ with a excitations ($a = 1, 2, \dots, N-1$), the equal-weight linear combination of all possible product states with the same number of excitations [cf. Eqs. (1) and (4)], is reachable in the system at hand provided that one starts from a generic product state with the Hamming weight a ; all such product states can succinctly be written in the form $P\{|1\rangle^{\otimes a}|0\rangle^{\otimes(N-a)}\}$, where P is an arbitrary permutation of the set $\{1, 2, \dots, N\}$. Therefore, if one starts from, e.g., the initial state

$$|\psi(t=0)\rangle = |1\rangle^{\otimes a}|0\rangle^{\otimes(N-a)} \equiv |\underbrace{11\dots 1}_{a} \underbrace{00\dots 0}_{N-a}\rangle, \quad (18)$$

then the above Lie-algebraic result guarantees that an appropriate time dependence of the field $B(t)$ can be found such that at a later time T the Dicke state $|D_a^N\rangle$ of the N -qubit array is engineered, i.e.

$$|\psi(t=T)\rangle = |D_a^N\rangle. \quad (19)$$

In this manner, the state $|D_a^N\rangle$ is dynamically generated within a time interval of duration T from an initial Hamming-weight- a product state [cf. Eq. (18)].

While, as explained above, the subspace controllability of the system holds for each of the three possible directions of $\mathbf{B}(t)$ [cf. Sec. IV B], Dicke states are eigenstates of the z projection S_z of the collective spin operator [cf. Eq. (15)], where the eigenvalue corresponding to the state $|D_a^N\rangle$ is given by $N/2 - a$. This is what makes the z direction special as far as Dicke states are concerned. Because of that, we will discuss dynamical generation of Dicke states with a local Z control on the first qubit (for an illustration, see Fig. 4), which constitutes one special realization of the family of the local-control Hamiltonians in Eq. (17). Therefore, the control part of the total system Hamiltonian will hereafter have the form $B(t)Z_1$. The total Hamiltonian of an N -qubit array is then given by

$$H(t) = J \sum_{n=1}^{N-1} (X_n X_{n+1} + Y_n Y_{n+1} + Z_n Z_{n+1}) + B(t)Z_1. \quad (20)$$

Needless to say, the appropriate time-dependence $B(t)$ of the control field that allows one to engineer the desired Dicke state within the shortest possible time – and this time T itself – do not follow from the above Lie-algebraic controllability/reachability results, but has to be determined by other means. To this end, the toolbox of quantum optimal control is utilized in what follows.

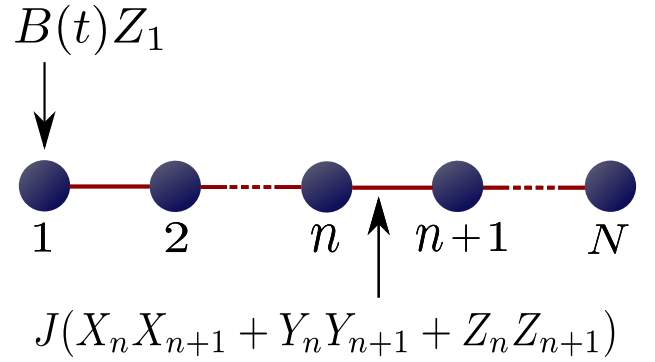


FIG. 4: Schematic illustration of an N -qubit array with nearest-neighbor isotropic Heisenberg interaction and a local Z control acting on the first qubit in the array.

In the following, the dynamical generation of Dicke states in a qubit array described by a Hamiltonian of Eq. (20) is investigated for array lengths up to $N = 9$, with the first qubit playing the role of actuator [i.e. $n_c = 1$ in Eq. (17)]. Therefore, the control objective is to find the shortest possible evolution time $T = T_{\min}$ that allows one to realize the desired Dicke state, as well as the corresponding (state-specific) time dependence of the control field $B(t)$. The control-field magnitude in the problem at hand will be expressed in units of the coupling strength J ; at the same time, all the relevant times will be expressed in units of J^{-1} (recall that $\hbar = 1$).

The Dicke-state generation problem under consideration is that of engineering a target state of a closed quantum system – up to an unimportant global phase – in a finite time T . Therefore, the relevant figure of merit in this problem is the target-state fidelity

$$\mathcal{F}_{t=T} = |\langle \psi(t=T) | D_a^N \rangle|^2, \quad (21)$$

i.e. the module squared of the overlap between the actual state $|\psi(t=T)\rangle$ of the system at time $t = T$ and the target Dicke state $|D_a^N\rangle$; the state $|\psi(t=T)\rangle$ is given by $U(t=T)|\psi(t=0)\rangle$, where $U(t)$ is the time-evolution operator of the system, i.e. the one corresponding to the Hamiltonian in Eq. (20) [for details of the numerical evaluation of $U(t)$, see Sec. (V B) below]. For each choice of the target Dicke state (i.e. for each different choice of N and a), the aim is to find the time dependence $B(t)$ of the control field that maximizes the state fidelity.

B. Quantum optimal-control schemes

In the following we describe the optimal-control approach employed here to determine the time dependence $B(t)$ of the control field that permits the realization of the desired Dicke states in an array with N qubits.

It is a common practice in quantum optimal control to start with piecewise-constant control fields [72]. In that case the time-evolution operator $U(t)$ of the system – describing its dynamics for $0 \leq t \leq T \equiv N_f \Delta t$ – is given by

a product of factors of the form $\exp[-i(H_0 + H_C^{(k)})\Delta t]$, which is characteristic of time-independent Hamiltonians; here H_0 is the drift Hamiltonian of the system and $H_C^{(k)}$ the (time-independent) control Hamiltonian during the k -th time interval of duration Δt ($k = 1, \dots, N_f$) in which the control field has a constant value B_k . Among the quantum optimal-control schemes that rely on piecewise-constant control fields, the most widely used one is based on the GRAPE (GRadient Ascent Pulse Engineering) algorithm [73], which iteratively updates the control-field values in each piecewise-constant step in order to maximize the relevant figure of merit; its efficiency can be substantially enhanced by making use of quasi-Newton- or Newton-type updates [74]. Other notable numerical method that employs piecewise-constant control fields is the Krotov algorithm [75], distinguished by its enhanced convergence properties. Similar to GRAPE, the Krotov algorithm belongs to the group of gradient-based, open-loop optimization methods. Finally, it is worthwhile to mention the recently proposed GEOFPE (GEOdesic Pulse Engineering) [79], which relies on differential programming and geodesics on the Riemannian manifold of $SU(2^N)$.

While working with piecewise-constant control fields has certain advantages, in this work we make use of smooth time-dependent control pulses. By contrast to the piecewise-constant case, in this continuous-wave approach to quantum optimal control the total system Hamiltonian $H(t)$ carries an explicit time dependence and, in general, does not commute with itself at different times, i.e. $[H(t'), H(t'')] \neq 0$. Consequently, the time-evolution operator of the system is given by the most general form, which entails a time-ordered exponential:

$$U(t) = \mathcal{T} \exp \left[-i \int_0^t H(t') dt' \right]. \quad (22)$$

Therefore, for a finite-time dynamical evolution of the system, such time-evolution operator ought to be determined by purely numerical means.

In addition to gradient-based algorithms for optimal control, there are also approaches that are not gradient-based and incorporate bandwidth limitation and smooth pulses in a few-parameter Ansatz. Examples of such approaches are furnished by the CRAB (Chopped RAnom Basis) formalism [76], which encodes pulses in a chopped randomized Fourier basis, as well as its improvement called dressed-CRAB (dCRAB) [77] (see the detailed description in Sec. V C below); another example for optimal-control algorithms of this class is GRAFS (GRadient Ascent in Function Space) [78], which places special emphasis on smooth control fields. Motivated by its superior convergence properties, enhanced compared to its parent CRAB algorithm, in the state-engineering problem at hand we employ the dCRAB algorithm [77].

C. dCRAB: a short description of the algorithm

In what follows, we describe the essential features of the dCRAB algorithm [77], along with some basic details of our own implementation thereof in the problem under consideration. These details include, e.g., our approach to global optimization – which is more advanced than the ones conventionally used in applications of the dCRAB formalism – as well as some quantitative details of our implementation (e.g. the chosen threshold value of the figure of merit, the number of dressing iterations, etc.).

The first issue in any application of the dCRAB formalism is the choice of the functional basis in which to parametrize the control fields. While, in principle, different bases can be employed in conjunction with the dCRAB formalism [80], we parametrize our smooth control pulses using a truncated randomized Fourier basis, i.e. a basis that consists of a finite number of sine- and cosine harmonics with randomly sampled frequencies. In this basis, the control field $B(t)$ is decomposed as

$$B(t) = \sum_{m=0}^{M-1} [c_m \cos(\omega_m t) + s_m \sin(\omega_m t)], \quad (23)$$

where ω_m are randomly chosen frequencies within a given interval; here, we take $\omega_m = 2\pi(m + r_m)/T$, where r_m is randomly sampled in the interval $[-0.5, 0.5]$ and T denotes the total evolution time. As a consequence of the dependence of the control field $B(t)$ on the parameters $\{c_0, c_1, \dots, c_{M-1}\}$ and $\{s_0, s_1, \dots, s_{M-1}\}$, the time-evolution operator $U(t)$ of the system is also a function of those parameters. By extension, the same is true of the state $|\psi(t = T)\rangle$ of the system at $t = T$ and the target-state infidelity $1 - \mathcal{F}_{t=T}$ [cf. Eq. (21)].

While the steps described up to now constitute the standard CRAB optimization, it is worthwhile taking into account that the basis has a finite number of degrees of freedom and the convergence may end in a non-optimal fixed point. The principal idea of dCRAB is then to dress the obtained pulse with new iterations of CRAB, namely by introducing a new pulse

$$\begin{aligned} B^{(l)}(t) = & B^{(l-1)}(t) + \\ & + \sum_{m=0}^{M-1} [c_m^{(l)} \cos(\omega_m^{(l)} t) + s_m^{(l)} \sin(\omega_m^{(l)} t)], \end{aligned} \quad (24)$$

where $\omega_m^{(l)}$ are newly sampled random frequencies, $B^{(l-1)}(t)$ denotes the pulse obtained at the previous CRAB iteration, and l enumerates repetitions of the dressing procedure. The optimization is performed once again, using $\{c_m^{(l)}, s_m^{(l)}\}$ as optimization parameters and keeping $B^{(l-1)}(t)$ fixed. The complete functional form of the pulse in the end reads

$$B(t) = \sum_{l=0}^{L-1} \sum_{m=0}^{M-1} [c_m^{(l)} \cos(\omega_m^{(l)} t) + s_m^{(l)} \sin(\omega_m^{(l)} t)], \quad (25)$$

where L denotes the total number of dressing iterations. Here, we set a maximum value of $L_{\max} = 10$, with the possibility of an early termination of the dressing procedure (hence, of the whole optimization as well) if the figure of merit is below a chosen threshold value (here $1 - \mathcal{F}_{t=T} = 10^{-3}$). We recall once again that, in the pulse parametrization of Eq. (25), the optimization parameters $\{c_m^{(l)}, s_m^{(l)}\}$ are not optimized for all at once, but for one value of l at a time.

We carry out local searches for the minima of the target-state infidelity $1 - \mathcal{F}_{t=T}$ [cf. Eq. (21)] using the Nelder-Mead method [47]. Moreover, to account for the complexity of the optimization landscape in the problem at hand, we also make use of the *multistart-based clustering* (also known as *multistart-based global random search*) algorithm [48]. The latter is widely used for finding global minima of objective functions that have a large number of very close local minima [81] and consists of the following steps. Firstly, one randomly selects a large ($\sim 10^3$) sample of points in the candidate-solution space. Secondly, one selects a much smaller (~ 20) number of points that yield the smallest values of the objective function (in the case at hand, the target-state infidelity) and performs local searches for minima around each of them; the one with the smallest value of the objective function is then adopted as the desired global minimum. The adequacy of this algorithm is corroborated by the stability of the obtained result for the global minimum of the objective function upon altering the number of random points in the initial step of the algorithm. Here, this strategy is used at the beginning of each dressing iteration, to obtain the best initial sample for global minimization.

The whole procedure described above allows the encoding of limited-bandwidth pulses and has already proven its effectiveness in realistic experimental settings [82]. We remark that, even if in the problem at hand the maximum bandwidth is tied to the value of M (i.e. increasing M increases the maximum frequency as well), nothing prevents from defining a given frequency interval $[\omega_{\min}, \omega_{\max}]$ and sampling M frequencies within it, hence allowing to freely change the number of degrees of freedom in the parametrization without affecting the targeted interval $[\omega_{\min}, \omega_{\max}]$.

The extent to which the use of time-dependent control fields can speed up a certain process depends on the control-field strength. For definiteness, in the problem at hand we assume that the control-field strength $B(t)$ (expressed in units of J) during the entire duration of control is within the range $[-4\pi, 4\pi]$. To account for this constraint in our numerical calculations, as the actual figure of merit we employ the target-state infidelity $1 - \mathcal{F}_{t=T}$ complemented with terms that account for the penalties incurred when the absolute value of $B(t)$ exceeds 4π , i.e.

$$\text{FoM} = 1 - \mathcal{F}_{t=T} + \Theta(B_{\max} - 4\pi)B_{\max} - \Theta(-4\pi - B_{\min})B_{\min}, \quad (26)$$

where Θ is the Heaviside function, $B_{\max} = \max_t B(t)$, and $B_{\min} = \min_t B(t)$.

VI. RESULTS AND DISCUSSION

In the following, we discuss our results obtained for Dicke- and W -state generation in Heisenberg-coupled arrays with up to $N = 9$ qubits and a local control field acting in the z direction on the first qubit in the array.

For each desired state, we minimized the figure of merit in Eq. (26) over the parameters $\{c_m^{(l)}, s_m^{(l)} | m = 0, \dots, M-1; l = 0, \dots, L-1\}$, for the varying total duration T of the pulse. For each target state, the total evolution time T is varied in small steps starting from an initial value, for which a high target-state fidelity cannot be achieved, until a high-fidelity realization of the desired target state becomes possible; the shortest time T for which a realization of the desired state within the assumed fidelity threshold ($1 - \mathcal{F}_{t=T} < 10^{-3}$) is possible is then identified with the shortest possible state-preparation time T_{\min} .

The results we obtained in the investigated examples of Dicke states, both for the genuine Dicke states ($a \geq 2$) and in the special case of W states ($a = 1$), are illustrated in Fig. 5. In particular, Fig. 5(a) contains the obtained shortest times T_{\min} required to realize particular Dicke states; these times are in the range between around J^{-1} (for the three-qubit W state) and around $10J^{-1}$ (for the nine-qubit W state). At the same time, Fig. 5(b) depicts the target-state infidelities achieved for $T = T_{\min}$ in the numerical optimization process; as can be inferred from

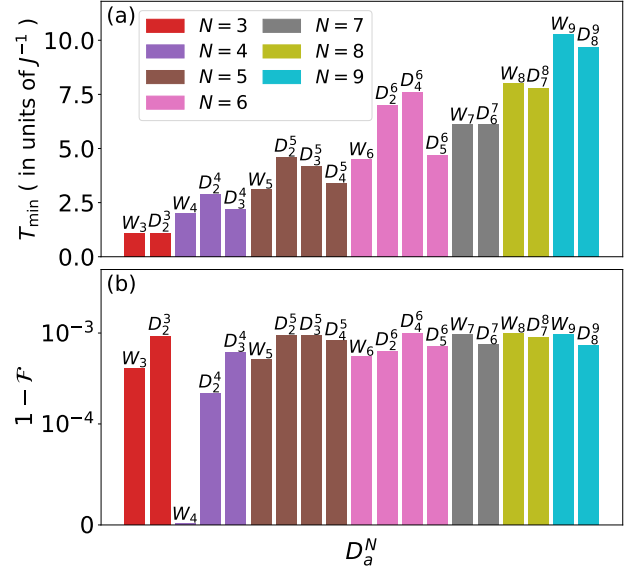


FIG. 5: Pictorial overview of the results obtained using the optimal-control approach based on the dCRAB formalism (with $M = 15$ harmonics in the truncated random Fourier basis) for an N -qubit array with isotropic, nearest-neighbor Heisenberg coupling and a Z control on the first qubit: (a) The shortest times T_{\min} required for the realization of Dicke states ($|D_a^N\rangle$) and W states ($|W_N\rangle$); (b) The highest fidelities achieved numerically for each of the investigated Dicke- and W states with an evolution of duration T_{\min} .

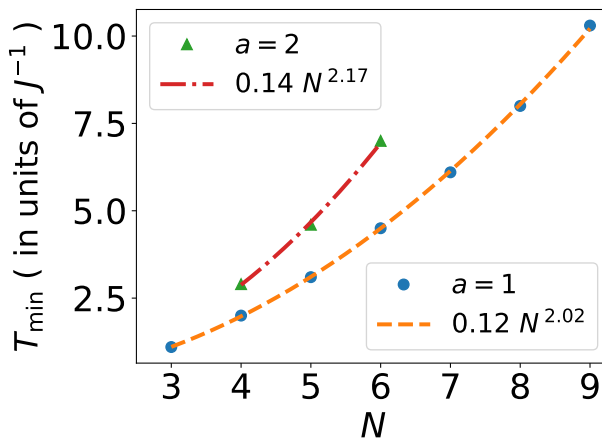


FIG. 6: Illustration of the scaling of the shortest possible state-preparation time T_{\min} , for both Dicke states $|D_a^N\rangle$ and W states ($a = 1$), with the number N of qubits. The displayed results are obtained using the dCRAB formalism, with $M = 15$ harmonics in the truncated random Fourier basis.

the plot, these infidelities are mostly between 10^{-3} and 10^{-4} .

Our optimal-control approach to engineering Dicke states $|D_a^N\rangle$ in an N -qubit array entails working in a basis of $\binom{N}{a}$ states – the dimension of the a -excitation subspace \mathcal{H}_a of the total 2^N -dimensional Hilbert space (recall Sec. IV B above). Because for fixed system size N the dimension of this subspace grows rapidly with increasing the excitation number a – before reaching the maximal value for $a = N/2$ or $a = \lfloor N/2 \rfloor$ – the problem becomes increasingly more difficult from the numerical standpoint. Therefore, it becomes increasingly difficult to engineer Dicke states for large values of N and values a close to $N/2$.

In order to assess the efficiency of the local-control approach in engineering highly-entangled multiqubit states for Heisenberg-coupled qubit arrays it is of interest to deduce the scaling of the state-preparation times T_{\min} with the number of qubits N . Based on our obtained numerical results, a fitting procedure aimed at extracting the power-law dependence $T_{\min}(N) \propto N^\alpha$ returns the result $T_{\min}(N) = 0.14 N^{2.17}$ for Dicke states $|D_2^N\rangle$ and $T_{\min}(N) = 0.12 N^{2.02}$ for the N -qubit W state. Therefore, the scaling of the shortest possible state-preparation time T_{\min} obtained using our optimal-control approach based on the dCRAB algorithm with N is – up to a small numerical deviation – quadratic in N for both classes of states (for an illustration, see Fig. 6).

It is pertinent at this point to comment on the obtained quadratic dependence of T_{\min} on N . It has become well-known by now that an overwhelming majority of the as yet proposed analog schemes for the Dicke-state preparation in various physical systems are characterized by state-preparation times that exhibit superlinear dependence on N [83, 84]. In this context, our obtained result $T_{\min}(N) \propto N^2$ represents a rather favorable scaling with

N . This is especially true given that this last result is obtained by means of what constitutes – from the controllability standpoint – the minimal possible control resource that allows the realization of the sought-after states in an entire class of systems (interacting qubit arrays) – a local Z control acting on a single actuator qubit. Needless to say, more conventional scenarios of quantum control in interacting qubit arrays either entail the use of global control fields [19] or time-dependent local control fields acting on each qubit in the array [85].

The characteristic time dependences of optimal control fields $B(t)$ that enable the realization of Dicke and W states are illustrated in Fig. 7. The examples shown correspond to the W states $|W_6\rangle, |W_7\rangle$ and Dicke states $|D_2^4\rangle, |D_4^5\rangle$; their respective state-preparation times are all in the range between $2.9 J^{-1}$ and $6.1 J^{-1}$. What can also be inferred from this plot is that the field strengths at all times $0 \leq t \leq T_{\min}$ indeed belong to the adopted maximal range $[-4\pi, 4\pi]$ of values. The fact that some of

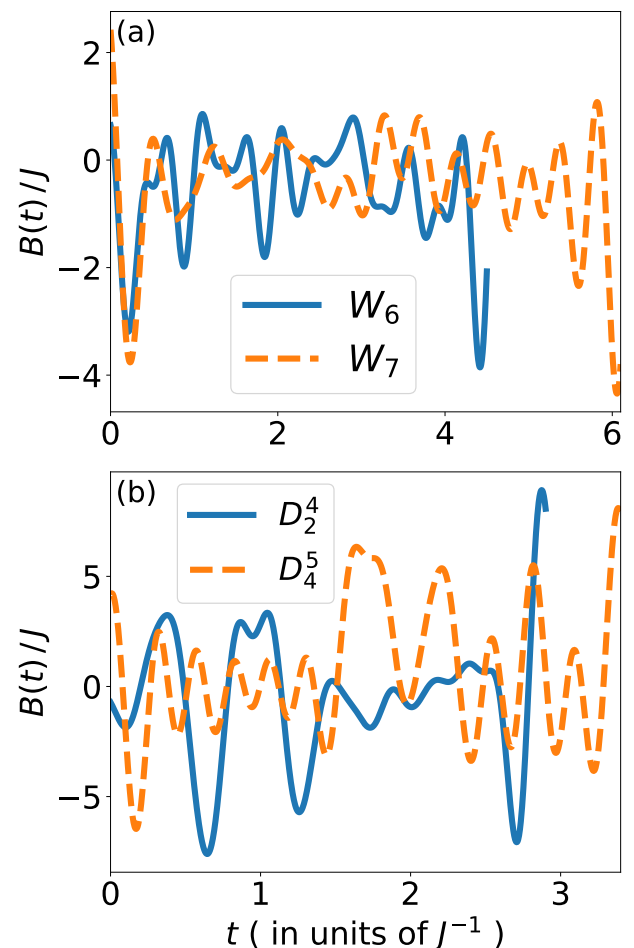


FIG. 7: Time-dependent control fields $B(t)$ that enable the optimal realization of (a) W states $|W_6\rangle$ and $|W_7\rangle$, and (b) Dicke states $|D_2^4\rangle$ and $|D_4^5\rangle$. These results are obtained using the dCRAB formalism, with $M = 15$ harmonics in the truncated random Fourier basis.

those fields reach values very close to the bounds of the adopted range underscores the importance of including the penalty terms in the generalized figure of merit [cf. Eq. (26)] that we utilize in this problem.

Regarding the practical feasibility of implementing rapidly varying control fields, such as those shown in Fig. 7, a comment is in order here. In present-day solid-state QC systems (based on superconducting- or spin qubits) operating in the microwave regime [64, 65], shaped control pulses are typically obtained using arbitrary waveform generators (AWGs); they are currently available with subnanosecond time resolutions. While in the conventional approach to control-pulse synthesis AWGs only generate a baseband signal and a sought-after pulse is obtained through an upconversion to microwave frequencies by mixing with a carrier, the very high sam-

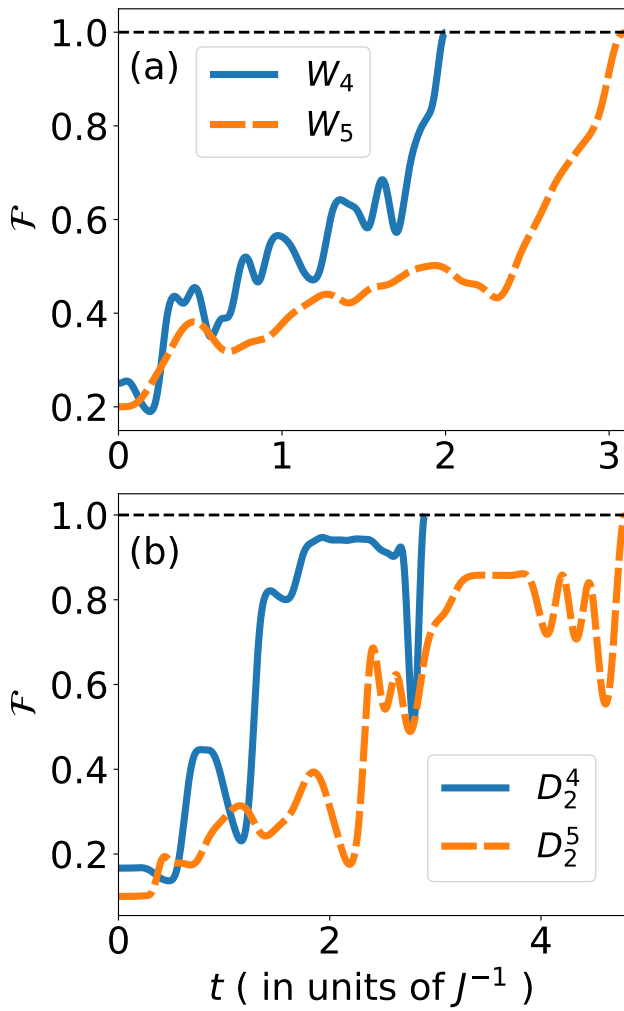


FIG. 8: Time dependence of the target-state fidelity $\mathcal{F}(t)$ throughout the dynamical evolution that starts from a Hamming-weight- a product state at $t = 0$ and ends with the Dicke- or W state at $t = T_{\min}$. The examples shown correspond to (a) W states $|W_4\rangle$ and $|W_5\rangle$, and (b) Dicke states $|D_2^4\rangle$ and $|D_2^5\rangle$.

pling rates of AWGs (~ 100 gigasamples per second) now allow direct digital synthesis of microwave pulses, obviating the need for additional microwave generators.

Figure 8 illustrates the time dependence of the state fidelity $\mathcal{F}(t)$ for both W - and genuine Dicke states. For the a -excitation Dicke state $|D_a^N\rangle$, the dynamical evolution starts from the Hamming-weight- a product state in Eq. (18); therefore, the initial value of the target-state fidelity is $\mathcal{F}_{t=0} = \binom{N}{a}^{-1}$. The fidelity has a rather complex time dependence before it reaches unity at $t = T_{\min}$.

In our numerical optimal-control calculations we utilize $M = 15$ harmonics in the truncated Fourier expansion of Eq. (23). Regarding the dependence of the obtained results on M , the following remark can be made. It transpires from our numerical calculations that the obtained results depend on M only in an implicit fashion. To be more specific, a sufficiently large value of M – i.e. a large enough number of harmonics in the expansion of the control field [cf. Eq. (23)] – is necessary for high-fidelity re-

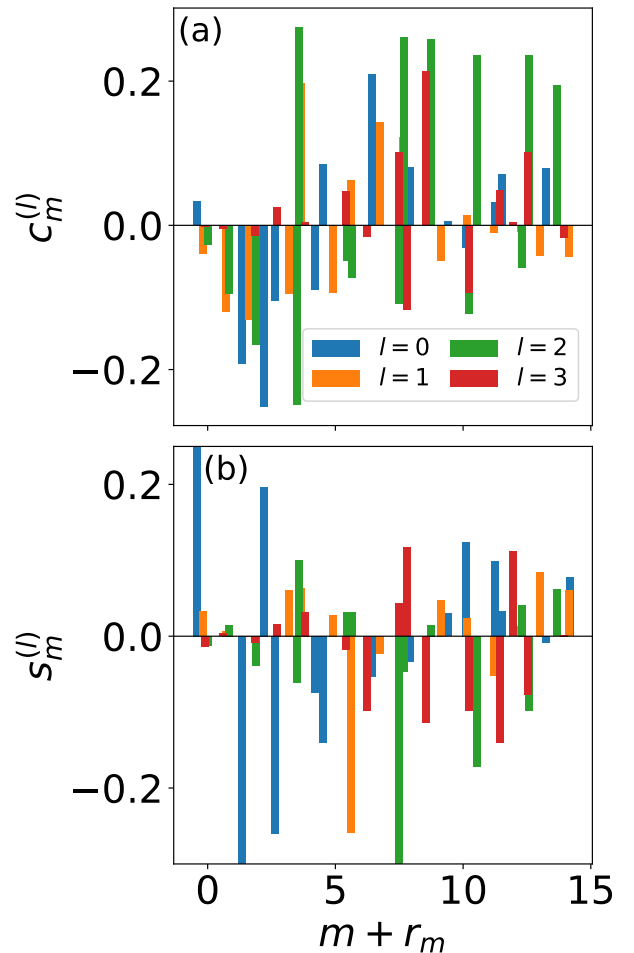


FIG. 9: Optimal parameters (a) $c_m^{(l)}$, and (b) $s_m^{(l)}$, obtained using the dCRAB formalism. The displayed results correspond to the state $|W_6\rangle$ and are obtained with $M = 15$ harmonics in the truncated random Fourier basis. Each color is associated to one specific value of l , i.e. one dressing iteration.

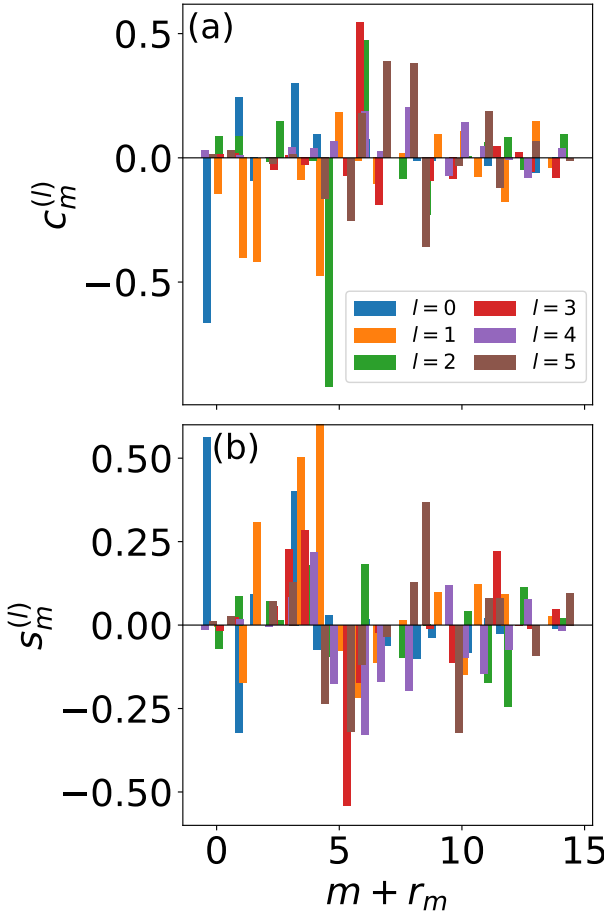


FIG. 10: Optimal parameters (a) $c_m^{(l)}$, and (b) $s_m^{(l)}$, obtained using the dCRAB formalism. The displayed results correspond to the state $|D_2^4\rangle$ and are obtained with $M = 15$ harmonics in the truncated random Fourier basis. Each color is associated to one specific value of l , i.e. one dressing iteration.

alizations of Dicke states; in particular, the states $|D_a^N\rangle$ that correspond to larger values of N and a cannot be successfully engineered if M is too small. However, provided that M is chosen to be sufficiently large (as is the case for $M = 15$ that we use in the problem under consideration), the actual minimal state-engineering times for different Dicke states do not show any dependence on M . This speaks in favor of the robustness of our dCRAB-based optimal-control approach.

In order to provide a further quantitative characterization of our implementation of the dCRAB formalism, it is instructive to look more closely into the parameters $c_m^{(l)}$ and $s_m^{(l)}$ ($l = 0, \dots, L-1$) resulting from the dressing iterations [cf. Sec. V C]. In Figs. 9 and 10 these parameters are displayed for the states $|W_6\rangle$ and $|D_2^4\rangle$, respectively. What can be inferred from these plots is that all dressing iterations [i.e. their corresponding optimization parameters $c_m^{(l)}$ and $s_m^{(l)}$ for $l = 1, \dots, L-1$] play an important role in the optimization process, not only the original optimization parameters $c_m^{(0)} \equiv c_m$ and $s_m^{(0)} \equiv s_m$

[i.e. coefficients in the original truncated random Fourier expansion of Eq. (25)]. This important conclusion constitutes an *a posteriori* justification for our use of the dCRAB formalism, i.e. our preference for this method rather than its parent CRAB method.

To end with, it is pertinent to provide a quantitative assessment of the robustness of our approach to Dicke-state engineering against errors in numerically-synthesized smooth control pulses. These errors will result from errors ε in the optimization parameters $c_m^{(l)}$ and $s_m^{(l)}$ ($m = 0, \dots, M-1; l = 0, \dots, L-1$).

In particular, Fig. 11 shows the deviations of the target-state fidelity from its optimal values due to errors in individual optimization parameters $c_m^{(l)}$ and $s_m^{(l)}$ (only a subset of all parameters is displayed). What can be inferred from the error-analysis reported through Fig. 11 is that errors as large as 5% in these parameters lead to errors in the fidelity of the order of 10^{-4} , which indicates that our approach is extremely robust to errors in

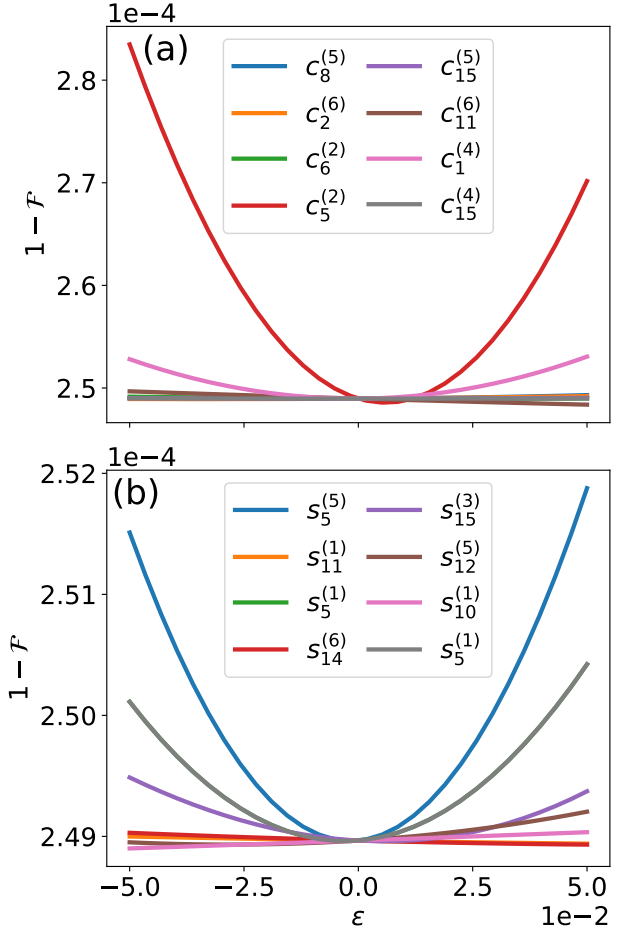


FIG. 11: Deviation from the optimal fidelity due to errors ε in individual optimization parameters (a) $c_m^{(l)}$, and (b) $s_m^{(l)}$, for select values of m and l . The results displayed here correspond to the state $|D_2^4\rangle$ realized using the dCRAB formalism with $M = 15$.

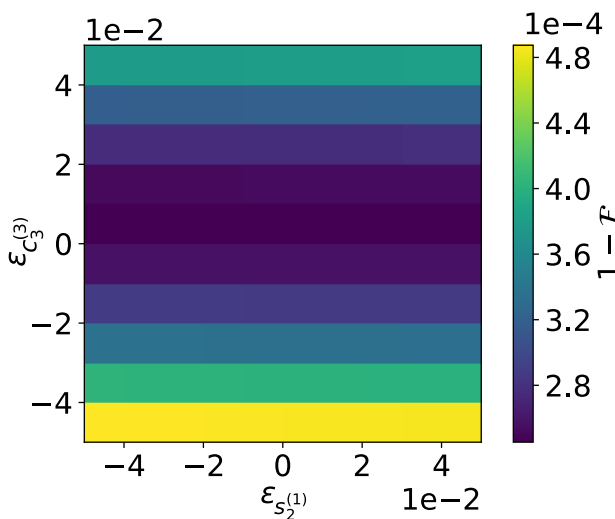


FIG. 12: Deviation from the optimal fidelity due to simultaneous errors ε in the optimization parameters $c_3^{(3)}$ and $s_2^{(1)}$. The results displayed here correspond to the state $|D_2^4\rangle$ realized using the dCRAB formalism with $M = 15$.

individual optimization parameters.

As a complement to Fig. 11, Fig. 12 illustrates the deviations of the target-state fidelity from its optimal values resulting from simultaneous errors in two different optimization parameters, more precisely $c_3^{(3)}$ and $s_2^{(1)}$. Once again, even simultaneously present errors as large as 5% in two different parameters lead to deviations in the fidelity that are only of the order of 10^{-4} . Along with similar results (not shown here) obtained for other pairs of optimization parameters, this demonstrates that our approach is extremely robust to simultaneous errors in more than one optimization parameters.

VII. SUMMARY AND CONCLUSIONS

In summary, the feasibility of time-efficient analog (single-shot) realizations of Dicke states was investigated in this paper for qubit arrays with the isotropic, nearest-neighbor Heisenberg coupling between qubits and a single Zeeman-type local (i.e. acting on a single actuator qubit) control in the z direction. The theoretical underpinning for the state-control scheme that permits en-

gineering of Dicke states $|D_a^N\rangle$ starting from a generic Hamming-weight- a product state is provided by an already proven, general result in the realm of Lie-algebraic controllability of interacting spin-1/2 chains (qubit arrays). This result guarantees the subspace controllability of Heisenberg-coupled qubit arrays on any subspace of the total N -qubit Hilbert space that is characterized by a fixed number of excitations (i.e. a fixed Hamming weight). This result implies – if a Z control is applied to a single qubit – that a time-dependent control field can be found that allows one to realize the Dicke state with the desired excitation number a starting from an arbitrary product state with the same number of excitations.

The problem of finding the appropriate time-dependence of the control field acting on an actuator qubit for engineering Dicke states – including W states as their special, single-excitation case – in the shortest possible time was addressed here for linear arrays with up to 9 qubits using methods of quantum optimal control. More specifically yet, the search for optimal, smoothly-varying control fields that enable the realization of Dicke states was carried out using the dCRAB algorithm in combination with advanced methods of global optimization. It was shown that the shortest time required for high-fidelity realizations of Dicke states in Heisenberg-coupled qubit arrays in this single-control setting scales quadratically with the number of qubits. To demonstrate the practical viability of the proposed local-control scheme, the robustness of the obtained results against various imperfections was also demonstrated.

To conclude, the present work underscores the potential usefulness of optimal-control schemes for engineering robust highly-entangled multiqubit states of interest for quantum-technology applications. In addition, it points to the utility of the local-control approach – i.e. the use of minimal control resources that permit the realization of a desired quantum-control task – in this context. Experimental realizations of such approaches, especially in the context of solid-state qubits, are clearly called for.

Acknowledgments

This research was supported in part by the Deutsche Forschungsgemeinschaft (DFG) – SFB 1119 – 236615297 (VMS).

[1] R. H. Dicke, Phys. Rev. **93**, 99 (1954).
[2] M. Bergmann and O. Gühne, J. Phys. A: Math. Theor. **46**, 385304 (2013).
[3] A. Neven, J. Martin, and T. Bastin, Phys. Rev. A **98**, 062335 (2018).
[4] W. Zhang, Z. Han, F. Shi, and X. Zhang, Phys. Rev. A **112**, 022408 (2025).
[5] D. A. Lidar and K. B. Whaley, in *Irreversible Quantum Dynamics* (Springer, Berlin Heidelberg, 2003), pp. 83–120.
[6] V. M. Stojanović and J. K. Nauth, Phys. Rev. A **108**, 012608 (2023).
[7] S. K. Özdemir, J. Shimamura, and N. Imoto, New J. Phys. **9**, 43 (2007).
[8] R. Prevedel, G. Cronenberg, M. S. Tame, M. Paternostro, P. Walther, M. S. Kim, and A. Zeilinger, Phys. Rev. Lett.

103, 020503 (2009).

[9] G. Toth, Phys. Rev. A **85**, 022322 (2012).

[10] Z. H. Saleem, M. Perlin, A. Shaji, and S. K. Gray, Phys. Rev. A **109**, 052615 (2024).

[11] See, e.g., Y. Ouyang, Phys. Rev. A **90**, 062317 (2014).

[12] See, e.g., J. Golden, A. Bärtschi, D. O’Malley, and S. Eidenbenz, Proc. IEEE Int. Conf. Quantum Comput. Eng., pp. 137 (2021).

[13] D. B. Hume, C. W. Chou, T. Rosenband, and D. J. Wineland, Phys. Rev. A **80**, 052302 (2009).

[14] P. A. Ivanov, D. Porras, S. S. Ivanov, and F. Schmidt-Kaler, J. Phys. B: At. Mol. Opt. Phys. **46**, 104003 (2013).

[15] L. Lamata, C. E. López, B. P. Lanyon, T. Bastin, J. C. Retamal, and E. Solano, Phys. Rev. A **87**, 032325 (2013).

[16] J. K. Stockton, R. van Handel, and H. Mabuchi, Phys. Rev. A **70**, 022106 (2004).

[17] Y.-F. Xiao, X.-B. Zou, and G.-C. Guo, Phys. Rev. A **75**, 012310 (2007).

[18] X.-Q. Shao, L. Chen, S. Zhang, Y.-F. Zhao, and K.-H. Yeon, EPL **90**, 50003 (2010).

[19] A. Muratori, V. M. Stojanović, E. Cuestas, T. Calarco, and F. Motzoi, arXiv:2512.19545.

[20] W. Wieczorek, R. Krischek, N. Kiesel, P. Michelberger, G. Toth, and H. Weinfurter, Phys. Rev. Lett. **103**, 020504 (2009).

[21] C. Wu, C. Guo, Y. Wang, G. Wang, X.-L. Feng, and J.-L. Chen, Phys. Rev. A **95**, 013845 (2017).

[22] T. Kobayashi, R. Ikuta1, S. Kaya Özdemir, M. Tame, T. Yamamoto, M. Koashi, and N. Imoto, New J. Phys. **16**, 023005 (2014).

[23] V. Jurdjević and H. J. Sussmann, J. Differ. Equations **12**, 313 (1972).

[24] G. M. Huang, T. J. Tarn, and J. W. Clark, J. Math. Phys. **24**, 2608 (1983).

[25] V. Ramakrishna and H. Rabitz, Phys. Rev. A **54**, 1715 (1996).

[26] D. D’Alessandro, *Introduction to Quantum Control and Dynamics* (Taylor & Francis, Boca Raton, 2008).

[27] C. P. Koch, U. Boscain, T. Calarco, G. Dirr, S. Filipp, S. J. Glaser, R. Kosloff, S. Montangero, T. Schulte-Herbrüggen, D. Sugny, and F. K. Wilhelm, EPJ Quantum Tech. **9**, 19 (2022).

[28] M. M. Müller, R. S. Said, F. Jelezko, T. Calarco, and S. Montangero, Rep. Prog. Phys. **85**, 076001 (2022).

[29] Q. Ansel, E. Dionis, F. Arrouas, B. Peaudecerf, S. Guerin, D. Guery-Odelin, and D. Sugny, J. Phys. B: At. Mol. Opt. Phys. **57**, 133001 (2024).

[30] For a recent review, see C. W. Duncan, P. M. Poggi, M. Bukov, N. T. Zinner, and S. Campbell, PRX Quantum **6**, 040201 (2025).

[31] P. Cappellaro, C. Ramanathan, and D. G. Cory, Phys. Rev. Lett. **99**, 250506 (2007).

[32] L. Stefanescu, L. Edwards-Pratt, J. O’Connor, E. Tsegaye, N. H. Le, and F. Mintert, Phys. Rev. A **112**, 012609 (2025).

[33] A. L. P. de Lima, J.-S. Li, L. S. Baker, A. Zlotnik, A. K. Harter, and M. J. Martin, arXiv:2511.01085.

[34] D. P. DiVincenzo, D. Bacon, J. Kempe, G. Burkard, and K. B. Whaley, Nature (London) **408**, 339 (2000).

[35] J. Levy, Phys. Rev. Lett. **89**, 147902 (2002).

[36] D. Bacon, J. Kempe, D. A. Lidar, and K. B. Whaley, Phys. Rev. Lett. **85**, 1758 (2000).

[37] T. Tanamoto, D. Becker, V. M. Stojanović, and C. Bruder, Phys. Rev. A **86**, 032327 (2012).

[38] See, e.g., T. Tanamoto, V. M. Stojanović, C. Bruder, and D. Becker, Phys. Rev. A **87**, 052305 (2013).

[39] S. G. Schirmer, I. C. H. Pullen, and P. J. Pemberton-Ross, Phys. Rev. A **78**, 062339 (2008).

[40] X. Wang, D. Burgarth, and S. G. Schirmer, Phys. Rev. A **94**, 052319 (2016).

[41] R. Heule, C. Bruder, D. Burgarth, and V. M. Stojanović, Phys. Rev. A **82**, 052333 (2010).

[42] Z. Zimboras, R. Zeier, T. Schulte-Herbrüggen, and D. Burgarth, Phys. Rev. A **92**, 042309 (2015).

[43] F. Albertini and D. D’Alessandro, Linear Algebra Appl. **705**, 207 (2025).

[44] R. Heule, C. Bruder, D. Burgarth, and V. M. Stojanović, Eur. Phys. J. D **63**, 41 (2011).

[45] V. M. Stojanović, Phys. Rev. A **99**, 012345 (2019).

[46] T. J. Green, J. Sastrawan, H. Uys, and M. J. Biercuk, New J. Phys. **15**, 095004 (2013).

[47] W. H. Press, S. A. Teukolsky, W. T. Vetterling, and B. P. Flannery, *Numerical Recipes in C: The Art of Scientific Computing* (Cambridge University Press, Cambridge, 1999).

[48] A. Törn and A. Žilinskas, *Global Optimization*, Lecture Notes in Computer Science, vol 350 (Springer, Berlin, 1989).

[49] V. M. Stojanović, Phys. Rev. Lett. **124**, 190504 (2020).

[50] V. M. Stojanović, Phys. Rev. A **103**, 022410 (2021).

[51] J. Zheng, J. Peng, P. Tang, F. Li, and N. Tan, Phys. Rev. A **105**, 062408 (2022).

[52] G. Q. Zhang, W. Feng, W. Xiong, Q. P. Su, and C. P. Yang, Phys. Rev. A **107**, 012410 (2023).

[53] V. M. Stojanović and J. K. Nauth, Phys. Rev. A **106**, 052613 (2022).

[54] E. Lötstedt and K. Yamanouchi, Phys. Rev. A **111**, 062416 (2025).

[55] T. Haase, G. Alber, and V. M. Stojanović, Phys. Rev. A **103**, 032427 (2021).

[56] T. Haase, G. Alber, and V. M. Stojanović, Phys. Rev. Res. **4**, 033087 (2022).

[57] J. K. Nauth and V. M. Stojanović, Phys. Rev. A **106**, 032605 (2022).

[58] A. Bärtschi and S. Eidenbenz, in *Fundamentals of Computation Theory, FCT 2019*, Lecture Notes in Computer Science, Vol. 11651, edited by L. A. Gasieniec, J. Jansson, and C. Levcopoulos (Springer International Publishing, Cham, 2019), pp. 126–139.

[59] A. Bärtschi and S. Eidenbenz, in *Proceedings of the 2022 IEEE International Conference on Quantum Computing and Engineering (QCE)*, Broomfield, CO, USA(IEEE, Piscataway, NJ, 2022), pp. 87–96.

[60] M. A. Nielsen and I. L. Chuang, *Quantum Computation and Quantum Information* (Cambridge University Press, Cambridge, 2000).

[61] W. Pfeifer, *The Lie Algebras $su(N)$: An Introduction* (Birkhäuser, Basel, 2003).

[62] See, e.g., S. Lorenzo, T. J. G. Apollaro, A. Sindona, and F. Plastina, Phys. Rev. A **87**, 042313 (2013).

[63] M. Veldhorst, H. G. J. Eeenink, C. H. Yang, and A. S. Dzurak, Nat. Commun. **8**, 1766 (2017).

[64] See, e.g., I. Hansen, A. E. Seedhouse, A. Saraiva, A. Laucht, A. S. Dzurak, and C. H. Yang, Phys. Rev. A **104**, 062415 (2021).

[65] H. C. George, M. T. Madzik, E. M. Henry, A. J. Wagner, M. M. Islam, F. Borjans, E. J. Connors, J. Corrigan, M.

Curry, M. K. Harper, *et al.*, *Nano Lett.* **25**, 793 (2025).

[66] J. Preskill, *Quantum* **2**, 79 (2018).

[67] J. Chen, Y. Zhou, J. Bian, J. Li, and X. Peng, *Phys. Rev. A* **102**, 032602 (2020).

[68] V. Evangelakos, E. Paspalakis, and D. Stefanatos, *Phys. Rev. A* **110**, 052601 (2024).

[69] D. Koutromanos, D. Stefanatos, and E. Paspalakis, *EPJ Quantum Technol.* **11**, 85 (2024).

[70] V. Evangelakos, E. Paspalakis, and D. Stefanatos, *Sci. Rep.*, in press (2025).

[71] See, e.g., S. S. Ivanov, P. A. Ivanov, I. E. Linington, and N. V. Vitanov, *Phys. Rev. A* **81**, 042328 (2010).

[72] V. M. Stojanović, A. Fedorov, A. Wallraff, and C. Bruder, *Phys. Rev. B* **85**, 054504 (2012).

[73] N. Khaneja, T. Reiss, C. Kehlet, T. Schulte-Herbrüggen, and S. J. Glaser, *J. Magn. Reson.* **172**, 296 (2005).

[74] P. de Fouquière, S. G. Schirmer, S. J. Glaser, and I. Kuprov, *J. Magn. Reson.*, **212**, 412 (2011).

[75] M. H. Goerz, D. Basilewitsch, F. Gago-Encinas, M. G. Krauss, K. P. Horn, D. M. Reich, and C. Koch, *SciPost Phys.* **7**, 080 (2019).

[76] T. Caneva, T. Calarco, and S. Montangero, *Phys. Rev. A* **84**, 022326 (2011).

[77] N. Rach, M. M. Müller, T. Calarco, and S. Montangero, *Phys. Rev. A* **92**, 062343 (2015).

[78] D. Lucarelli, *Phys. Rev. A* **97**, 062346 (2018).

[79] D. Lewis, R. Wiersema, and S. Bose, arXiv:2508.16029.

[80] A. Pagano, M. M. Müller, T. Calarco, S. Montangero, and P. Rembold, *Phys. Rev. A* **110**, 062608 (2024).

[81] V. M. Stojanović and M. Vanević, *Phys. Rev. B* **78**, 214301 (2008).

[82] A. Omran, H. Levine, A. Keesling, G. Semeghini, T. T. Wang, S. Ebadi, H. Bernien, A. S. Zibrov, H. Pichler, S. Choi, *et al.*, *Science* **365**, 570 (2019).

[83] T. Keating, C. H. Baldwin, Y.-Y. Jau, J. Lee, G. W. Biedermann, and I. H. Deutsch, *Phys. Rev. Lett.* **117**, 213601 (2016).

[84] M. T. Johnsson, N. R. Mukty, D. Burgarth, T. Volz, and G. K. Brennen, *Phys. Rev. Lett.* **125**, 190403 (2020).

[85] C. Arenz and H. Rabitz, *Phys. Rev. Lett.* **120**, 220503 (2018).